Original Article

Slowly progressive cell death induced by GPx4-deficiency occurs via MEK1/ERK2 activation as a downstream signal after iron-independent lipid peroxidation

Kahori Tsuruta,[1,2] Masaki Matsuoka,[1] Shinsaku Harada,[1] Ayaka Enomoto,[1] Takeshi Kumagai,[3] Shu Yasuda,[1] Tomoko Koumura,[1] Ken-ichi Yamada,[5] and Hirotaka Imai[1,4,*]

[1]Department of Hygienic Chemistry, [2]Laboratory of Microbiology, [3]Laboratory of Clinical Pharmacy Research, and [4]Medical Research Laboratories, School of Pharmaceutical Sciences, Kitasato University, 5-9-1 Shirokane, Minato-ku, Tokyo 108-8641, Japan
[5]Department of Molecular Pathobiology, Faculty of Pharmaceutical Sciences, Kyushu University, 3-1-1 Made, Higashi-ku, Fukuoka-shi, Fukuoka 812-8582, Japan

(Received 15 October, 2023; Accepted 28 October, 2023; Released online in J-STAGE as advance publication 1 November, 2023)

Glutathione peroxidase 4 (GPx4) is an antioxidant enzyme that reduces phospholipid hydroperoxide. Studies have reported that the loss of GPx4 activity through anticancer drugs leads to ferroptosis, an iron-dependent lipid peroxidation-induced cell death. In this study, we established Tamoxifen-inducible GPx4-deficient Mouse embryonic fibroblast (MEF) cells (ETK1 cells) and found that Tamoxifen-inducible gene disruption of GPx4 induces slow cell death at ~72 h. In contrast, RSL3- or erastin-induced ferroptosis occurred quickly within 24 h. Therefore, we investigated the differences in these mechanisms between GPx4 gene disruption-induced cell death and RSL3- or erastin-induced ferroptosis. We found that GPx4-deficiency induced lipid peroxidation at 24 h in Tamoxifen-treated ETK1 cells, which was not suppressed by iron chelators, although lipid peroxidation in RSL3- or erastin-treated cells induced ferroptosis that was inhibited by iron chelators. We revealed that GPx4-deficient cell death was MEK1-dependent but RSL3- or erastin-induced ferroptosis was not, although MEK1/2 inhibitors suppressed both GPx4-deficient cell death and RSL3- or erastin-induced ferroptosis. In GPx4-deficient cell death, the phosphorylation of MEK1/2 and ERK2 was observed 39 h after lipid peroxidation, but ERK1 was not phosphorylated. Selective inhibitors of ERK2 inhibited GPx4-deficient cell death but not in RSL3- or erastin-induced cell death. These findings suggest that iron-independent lipid peroxidation due to GPx4 disruption induced cell death via the activation of MEK1/ERK2 as a downstream signal of lipid peroxidation in Tamoxifen-treated ETK1 cells. This indicates that GPx4 gene disruption induces slow cell death and involves a different pathway from RSL3- and erastin-induced ferroptosis in ETK1 cells.

***Key Words*: iron, lipid peroxidation, GPx4, MEK1, ferroptosis**

Glutathione peroxidase 4 (GPx4) is an antioxidant enzyme that directly reduces phospholipid hydroperoxide (PLOOH) that is produced by reactive oxygen species using reduced glutathione (GSH). We previously reported that GPx4 knockout mice were embryonic lethal at 7.5 dpc[(1)] and were rescued by the GPx4-loxP transgenic (TG) genome.[(2)] Moreover, tissue-specific expression of Cre in these transgenic rescued GPx4-loxP TG/GPx4 KO mice [Tg(loxP-GPx4)$^{+/-}$:GPx4$^{-/-}$] could induce GPx4-deficient lipid peroxidation-derived cell death in the testis, photoreceptor cells, and heart.[(3–5)] In addition, we found that mouse embryonic fibroblast (MEF) cells isolated from GPx4-loxP TG/GPx4 KO mice [Tg(loxP-GPx4)$^{+/-}$:GPx4$^{-/-}$] underwent induced cell death slowly for 3 days due to GPx4-deficiency by disruption of GPx4-loxP-TG genome after infection with a retrovirus harboring Cre recombinase cDNA.[(2,3)] This GPx4-deficient cell death in MEF cells was rescued by the transfection of cytosolic GPx4 cDNA or the antioxidant Trolox, but not MnSOD or CuZnSOD cDNA, one of superoxide dismutases, as reported in 2009.[(2,3)] These results indicate that the depletion of GPx4 in normal tissues and cells induces lipid peroxidation-dependent cell death for 3 days after Cre expression. Similarly, Seiler *et al.*[(6)] established Tamoxifen-induced GPx4-deficient cells (Pfa1) and reported that cell death due to GPx4-deficiency was 15-lipoxygenase (15-LOX)-mediated and apoptosis inducing factor (AIF)-dependent in Pfa1 cells.

Ferroptosis was proposed as an oncogenic mutated RAS-selective Lethal (RSL)-induced non-apoptotic cell death that involves iron-dependent lipid peroxidation due to the loss of GPx4 activity.[(7,8)] RSL, such as erastin and RSL3, killed the engineered human tumor cells that expressed the oncogenic HRAS^{V12} at low concentrations but not the isogenic cells expressing the wild-type HRAS.[(9,10)] Erastin induces ferroptosis by inhibiting the Cystin transporter (xCT), which results in a decrease of glutathione and GPx4 activity.[(7)] Because RSL3 is directly bound to the GPx4 protein and inhibits GPx4 activity, GPx4-deficient cell death in Pfa1 cells and RSL3-induced ferroptosis are considered the same cell death type.[(8)] Erastin- or RSL3-induced ferroptosis at 24 h was inhibited by the iron chelator deferoxamine (DFO), antioxidant vitamin E, and ferrostatin-1 (Fer-1), thus indicating that ferroptosis is an iron-dependent lipid peroxidation-induced cell death. A number of molecules have been identified that regulate ferroptosis. Polyunsaturated fatty acids incorporated into phosphatidylethanolamine (PE) by Acyl-CoA synthetase long chain family member 4 (ACSL4) are directly oxidized by 15-LOX and become ferroptosis-inducing signals in Pfa1 cells.[(11,12)] Then, ferroptosis suppressor protein 1 (FSP1) is an enzyme that reduces ubiquinone and vitamin K, which are involved in the inhibition of lipid peroxidation and suppression of ferroptosis.[(13–15)] We previously reported that one of the factors in the pathogenesis of chronic obstructive pulmonary disease (COPD) is that cigarette smoke increases the expression of nuclear receptor coactivator 4 (NCOA4), which is involved in ferritinophagy for ferritin degradation, promotes iron

*To whom correspondence should be addressed.
E-mail: Imaih@pharm.kitasato-u.ac.jp

doi: 10.3164/jcbn.23-101

deposition, and suppresses the expression of GPx4, which results in the enhancement of ferroptosis in the lung epithelial cells.[16]

On the other hand, in doxorubicin cardiotoxicity, we have found that the inhibition of the expression of mitochondrial aminolevulinic acid synthase, a rate-limiting enzyme for heme synthesis, increased the iron in mitochondria and induced ferroptosis via lipid peroxidation through the doxorubicin-iron complex.[17,18] Thus, iron-mediated lipid peroxidation is closely related to pathogenesis through the promotion of ferroptosis.

However, although many molecules that inhibit or induce ferroptosis have been identified,[19,20] they mainly inhibit or enhance lipid peroxidation, and the factors that function downstream of this lipid peroxidation to induce cell death have not been elucidated.

In this study, we established Tamoxifen-induced GPx4-deficient cells (ETK1 cells) and analyzed the cell death upon the loss of GPx4. The results revealed that the loss of GPx4 through gene disruption induced cell death slowly at 72 h in a lipid peroxidation-dependent manner, compared to RSL3, a GPx4 inhibitor, which induced ferroptosis at 12 h. Analysis of the mechanisms of cell death induction over time revealed that lipid peroxidation peaks at 24 h, followed by the activation of the mitogen-activated protein kinase kinase 1 (MEK1)-extracellular signal-regulated kinase (ERK2) pathway around 40 h. This result is the first to demonstrate that lipid peroxidation does not directly induce cell death in GPx4-deficient cell death, but that there are factors that function downstream of lipid peroxidation. In addition, we found that in our established ETK1 cells, the lipid peroxidation process at 24 h was not mediated by the iron-induced Fenton reaction. This indicates that GPx4 gene disruption induces slow cell death and involves a different pathway from RSL3- and erastin-induced ferroptosis in ETK1 cells.

Materials and Methods

Reagents. U0126 was obtained from Cayman Chemical (Ann Arbor, MI). Fer-1, MEK inhibitor I, (Z)-4-hydroxytamoxifen (Tamoxifen), DFO, Trolox, and 3-methyladenine (3-MA) and erastin were obtained from Merck Millipore (Burlington, MA). RSL3, Z-VAD-FMK, and Ulixertinib were obtained from MedChemExpress (Monmouth Junction, NJ). Necrostatin 2 racemate (Nec-1s), pluripotin, and AZD0364 were obtained from Selleck Chemicals (Huston, TX). The chemical inhibitor library for several enzymes (SCADS inhibitor kits) was kindly gifted by the Molecular Profiling Committee.

Establishment of Tamoxifen-inducible GPx4 knockout (KO) MEF cells (ETK1 cells) and cell culture. As previously described,[2,3] MEF cells isolated from GPx4-loxP TG/GPx4 KO [Tg(loxP-GPx4)+/−:GPx4−/−] mice were immortalized through retrovirus infection with SV40 large T antigen produced by Ziptex (kindly gifted by Komada M). Cre-ERT2 cDNA (kindly gifted by Komada M) was introduced into pMx-Puro vector carrying a SV40-promoter-regulated puromycin-resistance gene. To establish Tamoxifen-inducible GPx4-deficient MEF cells, immortalized GPx4-loxP TG/GPx4 KO MEF cells (TK cells) were infected with a Cre-ERT2-SV40-Puro retrovirus produced from Plat-E cells (Cell Biolabs Inc., San Diego, CA), that was transfected with pMXs-Cre-ERT2-Puro vector and cultured for 7 days with 5 μg/ml puromycin.

We established Tamoxifen-inducible GPx4-deficient MEF cells [ETK1 cells; Cre-ERT2$^{+/-}$:Tg(loxP-GPx4)$^{+/-}$:GPx4$^{-/-}$] after cloning and screening to check for a decrease in GPx4 after the addition of (Z)-4-hydroxytamoxifen (Tamoxifen). ETK1 and Plat-E cells were cultured in DMEM (Nissui Pharmaceutical Co., Ltd., Tokyo, Japan) supplemented with 10% fetal bovine serum (Thermo Fisher Scientific, Waltham, MA) and 5 mg/ml Penicillin-Streptomycin-Glutamine (Thermo Fisher Scientific) at 37°C with 5% CO_2.

Knockdown and transduction of MEF cells by retroviral infection. Human GPx4 (hGPx4) cDNA and human MEK1 (hMEK1) cDNA were cloned by PCR using the primer sets listed below. hMEK1, and hGPx4 cDNA was cloned into the pMXs-IR vector for the overexpression, and the short hairpin RNA (shRNA) targeting sequence for MEK1 was inserted into piMG dr-U6 for knockdown. The Plat-E cells were seeded in 60 mm dishes at a density of 5×10^5 cells 24 h before transfection with 2 μg of plasmid DNA using Lipofectamine® Reagent (Thermo Fisher Scientific). The retrovirus produced by the Plat-E cells were transfected using pMXs-Puro Vector, pMXs-IRES-RFP (pMXs-IR)-based vectors, and piMG dr-U6. The virus supernatants were harvested after 48 h and centrifuged at 3,000 rpm for 15 min at 25°C.

MEF cells were seeded in 60 mm dishes at a density of 5×10^5 cells before transduction for 24 h, and the medium was replaced with 5 ml of retrovirus supernatant with 8 μg of polybrene (NACALAI TESQUE, INC., Kyoto, Japan). The targeting sequences used for knockdown were: MEK1; AGACCCTTC ACAGGCAGTGCATGCATGC. Primer sets used for hGPx4 cDNA, sense: 5'-ATAGAATTCCTGCTCTGTGGGGCTCTG-3', antisense: 5'-ATAGAATTCCACAAGGTAGCCAGGGGTG-3', and for hMEK1 cDNA, sense: 5'-ATTGGATCCGCGTTACCC GGGTCCAAAATGCC-3', antisense: 5'-CGCGGATCCGCTTCC CAAACACTTAGAGGC-3'.

Assessment of cell viability. For the induction of GPx4-depleted cell death, ETK1 cells were seeded in 6-well flat-bottom plates at a density of 2×10^4 cells/well for 24 h at 37°C in a CO_2 incubator. After incubation for 24 h, ETK1 cells were treated with 1 μM (Z)-4-hydroxytamoxifen (Tamoxifen) and cultured for a further 72 h. To test the cell growth rate, the number of cells was counted by taking 10 representative photos using an All-In-One Fluorescence Microscope (BZ-X810; KEYENCE, Osaka, Japan) at 0 h, 24 h, 48 h, and 72 h after adding Tamoxifen, and the cell growth rate was defined as the rate of increase in the number of adherent cells at each time point, with the number of adherent cells at 0 h set at 1. Cell viability (%) was estimated as a ratio of the number of adherent cells at 72 h after the addition of Tamoxifen with or without inhibitors (such as MEK inhibitor I, U0126, Trolox, Fer-1, DFO, Z-VAD-FMK, Necrostatin-1s, and 3-MA) compared to that of the no-treatment control. Cell viability (%) for the ERK inhibitors was calculated as the ratio of the number of cells at 72 h compared to the number of cells at 24 h after the addition of Tamoxifen. For ferroptosis induction, ETK1 cells were seeded in a 96-well flat-bottom plate at a density of 5×10^3 cells/well for 24 h at 37°C in a CO_2 incubator. After 24 h of incubation, ETK1 cells were treated with 1 μM RSL3 or 1 μM erastin with or without inhibitors. To test for cell viability, 5 μg 3-(4,5-Dimethyl-2-thiazolyl)-2,5-diphenyl-2H-tetrazolium Bromide (MTT) (Fujifilm-Wako, Osaka, Japan) was added to the culture medium for 3 h, and the formazan crystals that formed were solubilized by adding 100 μl of formazan lysis buffer [41% (v/v) *N*,*N*-dimethylfomamide, 2% (v/v) acetic acid, 0.216% (v/v) hydrochloric acid, 20% (w/v) SDS]. The absorbance intensity was measured using a Multiskan GO microplate reader (Thermo Fisher Scientific) at 570 nm. Cell viability (%) was estimated as a ratio of absorbance of MTT without ferroptosis induders at 24 h after the addition of ferroptosis inducers with or without inhibitors. Experiments were performed in triplicate, and the values are expressed as the mean ± SD.

Immunoblot analysis. The lysate sample was mixed with 3 × SDS buffer [67 mM Tris-HCl (pH 6.8)/5% (w/v) Glycerol/3% (w/v) SDS/2% (v/v) 2-mercaptoethanol] and heat-denatured. The lysate samples were then separated by sodium dodecyl sulfate-polyacrylamide gel electrophoresis and transferred to a polyvinylidene difluoride membrane (Merck Millipore). The membrane was blocked in 4% (w/v) skim milk (NACALAI

doi: 10.3164/jcbn.23-101

TESQUE, INC.) in tris-buffered saline containing 0.05% (v/v) Tween-20 (T-TBS), and reacted with the primary antibody in T-TBS. The membrane was then washed and reacted with the secondary antibody. The immunoreactive proteins on the membrane were detected using Chemi-Lumi One L (NACALAI TESQUE, INC.) and the ChemiDoc Touch imaging system (Bio-Rad Laboratories, Hercules, CA). The antibodies that were used for immunoblotting were: Anti-GPx4 mAb; 6F10, which we previously produced ourselves,[21] p-MEK1/2; phosphor-MEK1/2 (Ser217/221) rabbit polyclonal antibody (Cell Signaling Technology, Inc., Danvers, MA), Anti-MEK1; MEK1 (C-18) rabbit polyclonal antibody (Santa Cruz Biotechnology, Inc., Dallas, CA), Anti-MEK2; MEK2 (N-20) rabbit polyclonal antibody (Santa Cruz Biotechnology, Inc.), Anti-ERK1/2; p44/42 MAPK (Erk1/2) rabbit polyclonal antibody (Cell Signaling Technology, Inc.), Anti-p-ERK1/2; phosphor-p44/42 MAPK (Erk1/2) (Thr202/Tyr204) (D13.14.4E) XP® rabbi monoclonal antibody (Cell Signaling Technology, Inc.), Anti-β-actin; β-actin rabbit polyclonal antibody (Cell Signaling Technology, Inc.), Anti-rabbit goat anti-rabbit IgG H+L (HRP, horse radish peroxidase) (Cell Signaling Technology, Inc.), Anti-mouse sheep anti-mouse IgG (HRP) (GE Healthcare, Chicago, IL).

Detection of lipid peroxidation by flow cytometric analysis. ETK1 cells were seeded at 1×10^5/100 mm dish for Tamoxifen and 8×10^5 cells/100 mm dish for RSL3 or erastin and cultured in a 5% CO_2 incubator for 24 h. The cells were then treated with or without 1 μM Tamoxifen, 1 μM RSL3, or 1 μM erastin for 24 h, 3 h, and 7 h, respectively. To observe the effect of the inhibitors, the cells were incubated with or without 10 μM U0126, 600 μM Trolox, and 100 μM DFO for 3 h with RSL3, for 7 h with erastin, or for 24 h with Tamoxifen. To detect lipid peroxidation in the cells, 1 μM NBD-Pen (gifted kindly by KY), a detector of lipid radicals, as previously reported[22] or 4 μM BODIPY™ 581/591 C11 (D3861; Thermo Fisher) was added. After incubation for 30 min, the cells were collected with a cell scraper and centrifuged at 1,500 rpm for 10 min after the addition of PBS and analyzed with a MoFloTM XDP Flow Cytometer (Beckman Coulter, Inc., Brea, CA), and the data was then analyzed using Summit software ver. 5.3.1.12636.

Statistical analysis. The results of three independent replicate experiments were expressed as mean ± SEM. One-way analysis of variance and Students's unpaired *t* test were used for statistical comparison of the groups. $P<0.05$ was considered statically significant. Representative results were shown for the cell death images and immunoblot analysis.

Result

Establishment and characterization of Tamoxifen-inducible GPx4 deficient cells (ETK1 cells). We previously reported that the depletion of GPx4 through the infection with a Cre harboring retrovirus induced cell death for 3 days in the MEF (TK) cells obtained from GPx4-loxP transgene (TG)/GPx4 KO mice [Tg(loxP-GPx4)$^{+/-}$:GPx4$^{-/-}$], and the addition of Trolox, a vitamin E derivative, rescued the cell death induced by the retrovirus-Cre-mediated disruption of GPx4-loxP TG genome.[2,3] In this study, to elucidate the details of cell death upon loss of GPx4 through the GPx4-loxP transgene disruption, tamoxifen-induced GPx4-deficient cells [ETK1 cells; CRE-ERT2$^{+/-}$:Tg(loxP-GPx4)$^{+/-}$:GPx4$^{-/-}$] were established by transfection of CRE-ERT2 cDNA into immortalized GPx4-loxP TG/GPx4 KO MEF cells [Tg(loxP-GPx4)$^{+/-}$:GPx4$^{-/-}$]. The addition of Tamoxifen causes the cells to proliferate for up to 24 h but slowly induces cell death at 72 h in ETK1 cells (Fig. 1A and B). Furthermore, treatment with Trolox also rescued the cell death through the depletion of GPx4 (Fig. 1A and B). Immunoblot analysis revealed that the expression of GPx4 was reduced to about 20% at 24 h and 0.5% at 48 h of the control after the addition of Tamoxifen (Fig. 1C). When human GPx4 cDNA was introduced into ETK1 cells through retroviral infection, GPx4 expression in ETK1-hGPx4 cells increased 12-fold in the ETK1 cells (Fig. 1D). Retroviral transfection of human GPx4 expression completely rescued the cell death caused by Tamoxifen-inducible mouse GPx4 genome disruption (Fig. 1E), These results indicate that the loss of GPx4 at 24 h after the addition of Tamoxifen slowly induced cell death for 3 days in Tamoxifen-inducible GPx4-deficient cells (ETK1 cells), which was similar to the previously reported retroviral Cre expression system.[2,3]

Comparison between RSL3- or erastin-induced ferroptosis and Tamoxifen-inducible GPx4-deficient cell death in ETK1 cells. RSL3 (a GPx4 inhibitor) and erastin (an xCT transporter inhibitor) are known to induce ferroptosis, an iron-dependent lipid peroxidation-derived cell death.[7,8] We confirmed that the addition of RSL3 and erastin in ETK1 cells induced rapid cell death within 12 and 24 h, respectively in ETK1 cells (Fig. 1F). Overexpression of human GPx4 completely rescued cell death by erastin but could only partially rescue RSL3-induced ferroptosis (Fig. 1G and H).

Cell death through GPx4 genome disruption occurs slowly at 72 h in ETK1 cells (Fig. 1A), whereas RSL3 quickly induces cell death at 12 h (Fig. 1F). Therefore, we investigated whether cell death through Tamoxifen-inducible GPx4 genome disruption and ferroptosis by RSL3 or erastin are the same cell death mechanisms using a ferroptosis inhibitor.

Ferroptosis is inhibited by iron chelators such as DFO and antioxidants, such as Trolox and Fer-1.[7,8] RSL3- and erastin-induced ferroptosis in ETK1 cells at 24 h was markedly inhibited by 100 μM DFO, 300 μM Trolox, and 1 μM Fer-1 (Fig. 2A and B). On the other hand, Tamoxifen-inducible GPx4-deficient cell death was also markedly rescued by 300 μM Trolox and 1 μM Fer-1 at 72 h (Fig. 2C).

The inhibitory effect of 100 μM DFO on GPx4-deficient cell death after 72 h could not be evaluated because treatment with only 100 μM DFO for 48 and 72 h induced cell death in ETK1 cells. The addition of 100 μM DFO at 24 h and 36 h after the addition of Tamoxifen did not inhibit GPx4-deficient cell death. We then determined the DFO concentration that would not induce cell death until 72 h and found that 2.5 μM DFO treatment for 72 h showed no cytotoxicity, but 5 μM DFO treatment reduced viability to 75% (Fig. 2D). On the other hand, 5 μM DFO treatment at 72 h inhibited the Tamoxifen-inducible GPx4-deficient cell death by about 20% (Fig. 2D). This inhibitory effect of DFO on GPx4-deficient cell death was considerably less than the inhibitory effect of DFO on RSL3- or erastin-induced ferroptosis. Treatment with 5 μM DFO did not suppress the RSL3-induced ferroptosis at 24 h (Fig. 2E). A detailed analysis remains to be performed as to why low concentrations of DFO can weakly inhibit GPx4-deficient cell death. Besides, we determined whether Tamoxifen-inducible GPx4-deficient cell death is any other known type of cell death such as apoptosis, necroptosis, or autophagic cell death, using specific inhibitors. Tamoxifen-inducible GPx4-deficient cell death was not rescued by the necroptosis inhibitor, necrostatin-1s, or the autophagic cell death inhibitor, 3-methyladenine (3-MA) (Fig. 2F). Tamoxifen-inducible GPx4-deficient cell death was inhibited by the apoptosis inhibitor (Z-VAD-FMK) to a significant degree, but the inhibitory effect was also significantly weaker than that of the antioxidant Trolox (Fig. 2F). These results indicate that Tamoxifen-induced GPx4-deficient cell death is mainly lipid peroxidation-dependent and distinct from apoptosis, necrosis, and autophagic cell death.

Tamoxifen-inducible GPx4-deficient cell death in ETK1 cells is an iron-independent lipid peroxidation-induced cell death, but it is not ferroptosis. It is known that lipid peroxidation is enhanced by iron-mediated Fenton reactions in RSL3- and erastin-induced ferroptosis.[7,8] Tamoxifen-induced GPx4-

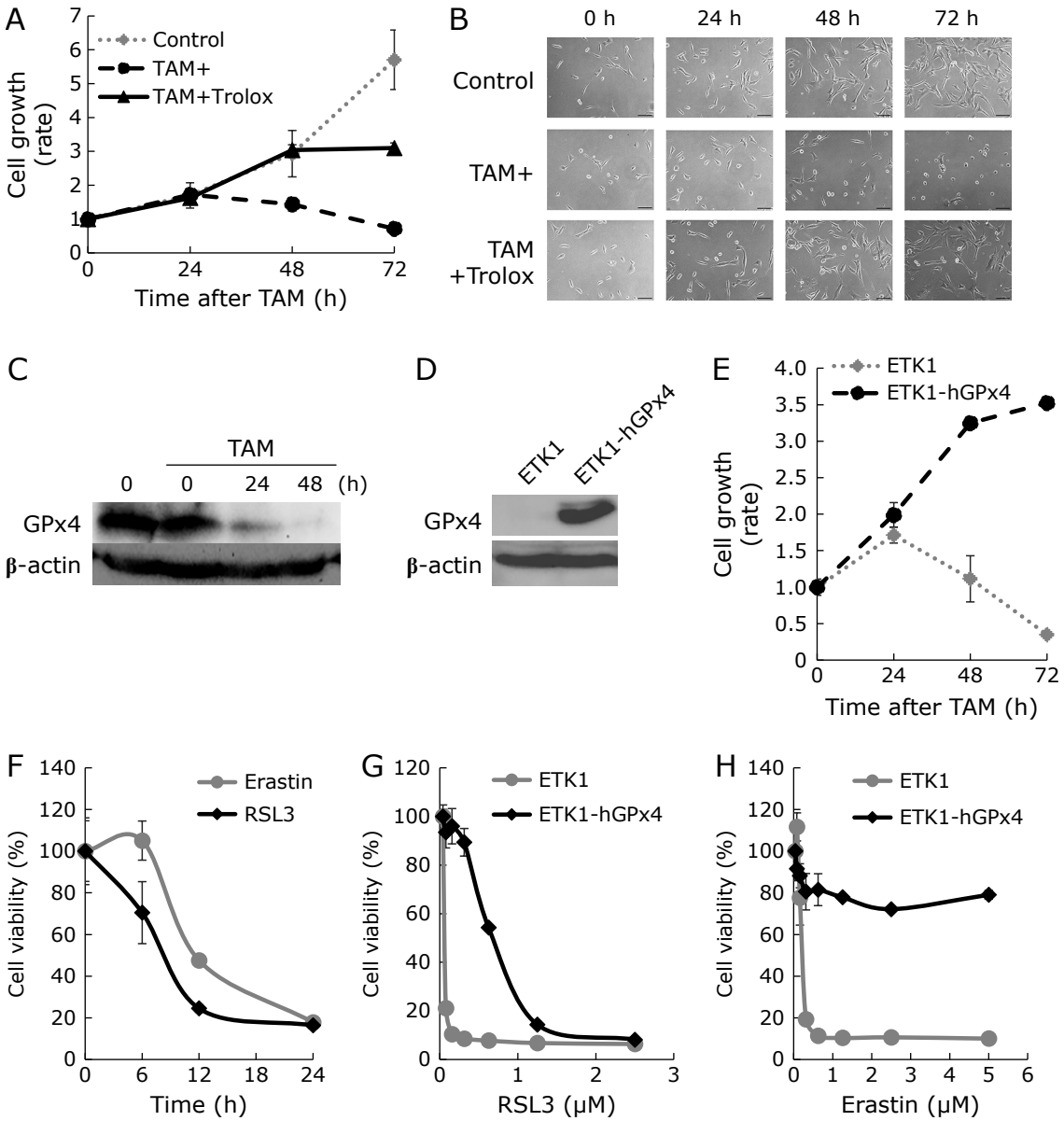

Fig. 1. GPx4-deficient cell death through GPx4 gene disruption and RSL3- and erastin-induced ferroptosis in Tamoxifen-inducible GPx4-deficient cells (ETK1 cells). Cell growth rates (A) and representative images (B) of Tamoxifen-inducible GPx4-deficient (ETK1) cells with the addition of 1 μM Tamoxifen (TAM) with or without 300 μM Trolox every 24 h. Tamoxifen-induced cell death occurs in 48 to 72 h. The scale indicates 100 μm. (C) Decrease of the expression of GPx4 at 24 h and 48 h in 1 μM Tamoxifen (TAM)-treated ETK1 cells through immunoblot analysis. (D) Expression of GPx4 in human GPx4-overexpressing ETK1 cells (ETK-hGPx4) through retroviral infection. (E) Retroviral transfection of human GPx4 into ETK1 cells completely inhibited the cell death caused by mouse GPx4 loss with the addition of Tamoxifen. (F–H) RSL3- and erastin-induced ferroptosis in ETK1 and ETK1-hGPx4 cells. (F) Time course of 1 μM RSL3- and 1 μM erastin-induced ferroptosis in ETK1 cells. (G, H) Different concentrations of RSL3 (G) and erastin (H) induced ferroptosis in ETK1 and ETK-hGPx4 cells. Cell viability was measured 24 h after treatment with 1 μM RSL3 (G) and 1 μM erastin (H).

deficient cell death is also lipid peroxidation-dependent because it is suppressed by Trolox and Fer-1, which inhibit lipid peroxidation (Fig. 1A and 2C). We examined whether the lipid peroxidation caused by Tamoxifen-inducible GPx4-deficiency was iron-dependent in ETK1 cells. We first examined the timing of lipid peroxidation using C11-BODIPY, a fluorescent probe for lipid peroxidation, in the Tamoxifen-inducible GPx4-deficient cell death of ETK1 cells. Lipid peroxidation was detected 12 h after the addition of Tamoxifen, reached a plateau at 24 h, and remained unchanged at 36 h (Fig. 3A). Additionally, we observed that lipid peroxidation was induced at 3 h and 7 h after the addition of RSL3 and erastin, respectively, in ETK1 cells by flow cytometric analysis using the lipid radical detection fluorescent probe NBD-Pen (Fig. 3C and D). We investigated whether lipid peroxidation was inhibited by iron chelators (DFO) or antioxidants (Trolox) in Tamoxifen-inducible GPx4-deficient cell death or RSL3- and erastin-induced ferroptosis by flow cytometric analysis using NBD-Pen. Treatment with 100 μM DFO or 600 μM Trolox for 24 h does not cause cytotoxicity in ETK1 cells (data not shown). RSL3- and erastin-induced lipid peroxidation were completely inhibited with 600 μM Trolox antioxidant treatment and 100 μM DFO iron-chelator treatment, indicating that lipid peroxidation generated by RSL3 at 3 h (Fig. 3C and F) and erastin at 7 h (Fig. 3D and G) was iron-dependent. On the

doi: 10.3164/jcbn.23-101

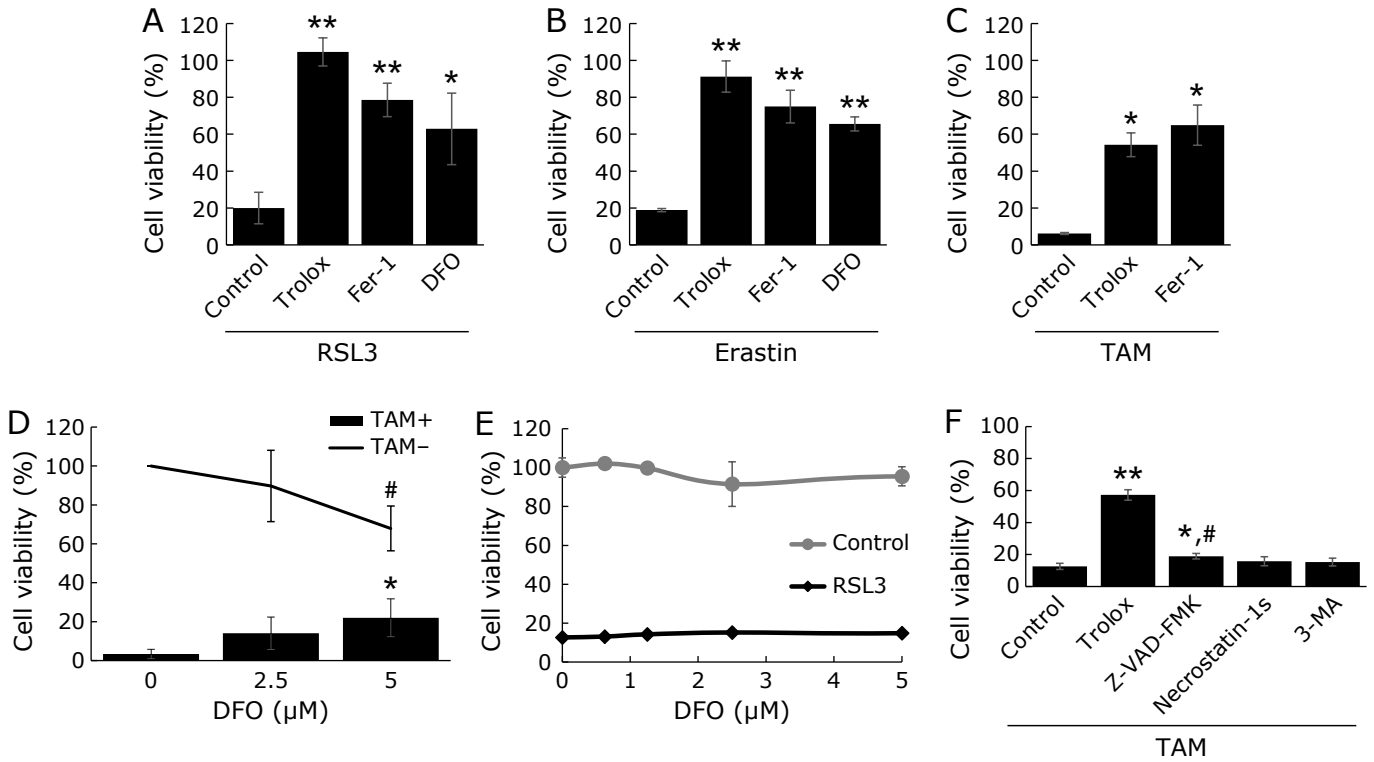

Fig. 2. Effects of ferroptosis inhibitors on RSL3- or erastin-induced ferroptosis and GPx4-deficient cell death in ETK1 cells. (A, B) Effect of Trolox, Ferrostatin-1 (Fer-1), and DFO on RSL3- (A) and erastin-(B) induced ferroptosis. Cell viability was assessed 24 h after the addition of 1 μM RSL3 (A) or 1 μM erastin (B) with or without 300 μM Trolox, 1 μM Fer-1, and 100 μM DFO in ETK1 cells. *p<0.05 vs RSL3- or erastin-treated ETK1 cells with no inhibitor (control), **p<0.01 vs RSL3- or erastin-treated ETK1 cells with no inhibitor (control). (C, D) Effect of Trolox, Fer-1, and DFO on Tamoxifen-inducible GPx4-deficient cell death in ETK1 cells. (C) Effect of Trolox and Fer-1 on Tamoxifen-inducible GPx4-deficient cell death in ETK1 cells. Cell viability was assessed 72 h after the addition of 1 μM Tamoxifen (TAM) with or without 300 μM Trolox and 1 μM Fer-1. (D) Effect of DFO on Tamoxifen-inducible GPx4-deficient cell death in ETK1 cells. Cell viability (bar graphs, TAM+) was assessed 72 h after the addition of 1 μM Tamoxifen (TAM) with or without 2.5 μM and 5 μM DFO and Line (TAM–) represent the cell viability (toxicity) when only 2.5 μM and 5 μM DFO are added and cultured for 72 h in ETK1 cells. The values represent the mean ± SE (each group, n = 3). *p<0.05 vs TAM treated ETK1 cells with no inhibitor (control), $^{\#}p$<0.05 vs ETK1 cells with no inhibitor (control). (E) Effect of low concentrations of DFO on RSL3-induced ferroptosis. Cell viability was assessed 24 h after the simultaneous addition of RSL3 with various concentrations of DFO. Controls represent the cell viability (toxicity) when only various concentrations of DFO are added and cultured for 24 h. The values represent the mean ± SE (each group, n = 3). (F) Effect of known cell death inhibitors on Tamoxifen-inducible GPx4-deficient cell death in ETK1 cells. Cell viability was assessed 72 h after the addition of 1 μM Tamoxifen (TAM) to ETK1 cells with 300 μM Trolox, 50 μM Z-VAD-FMK, 100 μM Necrostatin-1S, and 2.5 mM 3-Methyladenine (3-MA). The values represent the mean ± SE (each group, n = 3). *p<0.05 vs TAM treated ETK1 cells with no inhibitor (control), **p<0.01 vs TAM treated ETK1 cells with no inhibitor (control). $^{\#}p$<0.05 vs TAM treated ETK1 cells with Trolox (Trolox).

other hand, lipid peroxidation at 24 h in Tamoxifen-inducible GPx4-depleted cell death was suppressed by 600 μM Trolox, but not by 100 μM DFO, which indicates that lipid peroxidation through GPx4 gene disruption is iron-independent (Fig. 3B and E). These results indicate that RSL3- and erastin-induced ferroptosis and GPx4-deficient cell death are caused by different mechanisms of lipid peroxidation in our established ETK1 cells.

MEK1 is required for GPx4-deficient iron-independent lipid peroxidation-induced cell death in ETK1 cells. To clarify the mechanism of iron-independent lipid peroxidation-induced cell death through GPx4 gene disruption, we screened a chemical inhibitor library against several enzymes (SCADS inhibitor kits I~III) to suppress Tamoxifen-induced GPx4-deficient cell death. We found that the MEK 1/2 inhibitor, MEK inhibitor I (Fig. 4A), and U0126 (Fig. 4B) inhibited Tamoxifen-induced GPx4-deficient cell death in a dose-dependent manner (Fig. 4A and B). On the other hand, U0126 and MEK inhibitor I also suppressed the RSL3- and erastin-induced ferroptosis in a dose-dependent manner without toxicity (Fig. 4C and D). To investigate the requirement of MEK1 for Tamoxifen-induced GPx4-deficient cell death and RSL3- or erastin-induced ferroptosis, we established MEK1 knockdown (KD) cells through retrovirus infection harboring MEKI shRNA into ETK1 cells (Fig. 4E). Interestingly, MEK1 KD suppressed Tamoxifen-induced GPx4-deficient cell death (Fig. 4F and G), but not RSL3- or erastin-induced ferroptosis (Fig. 4H). Moreover, re-transfection of human MEK1 cDNA into MEK1 KD cells caused Tamoxifen-inducible GPx4-deficient cell death (Fig. 4E–G), thus indicating that MEK1 functions selectively as an executor in Tamoxifen-inducible GPx4-deficient cells in ETK1 cells.

MEK1/ERK2 pathway was involved after lipid peroxidation in Tamoxifen-inducible GPx4-deficient cell death in ETK1 cells. We investigated whether U0126, an MEK inhibitor, could inhibit cell death before or after lipid peroxidation in ETK1 cells using flow cytometric analysis with NBD-Pen, a lipid radical detector.[22] Lipid peroxidation was slightly enhanced by the addition of U0126 at 3 h. The enhancement of lipid peroxidation by the addition of RSL3, a ferroptosis inducer, was significantly inhibited by the simultaneous addition of U0126 in ETK1 cells (Fig. 5A). On the other hand, in Tamoxifen-inducible GPx4-deficient cell death, the lipid peroxidation at 24 h after the addition of Tamoxifen was not inhibited by the simultaneous treatment with U0126 (Fig. 5B). These results suggest that MEK1 functions after lipid peroxidation at 24 h in Tamoxifen-inducible GPx4-deficient cells. To determine that MEK is activated after lipid peroxidation at 24 h in Tamoxifen-inducible

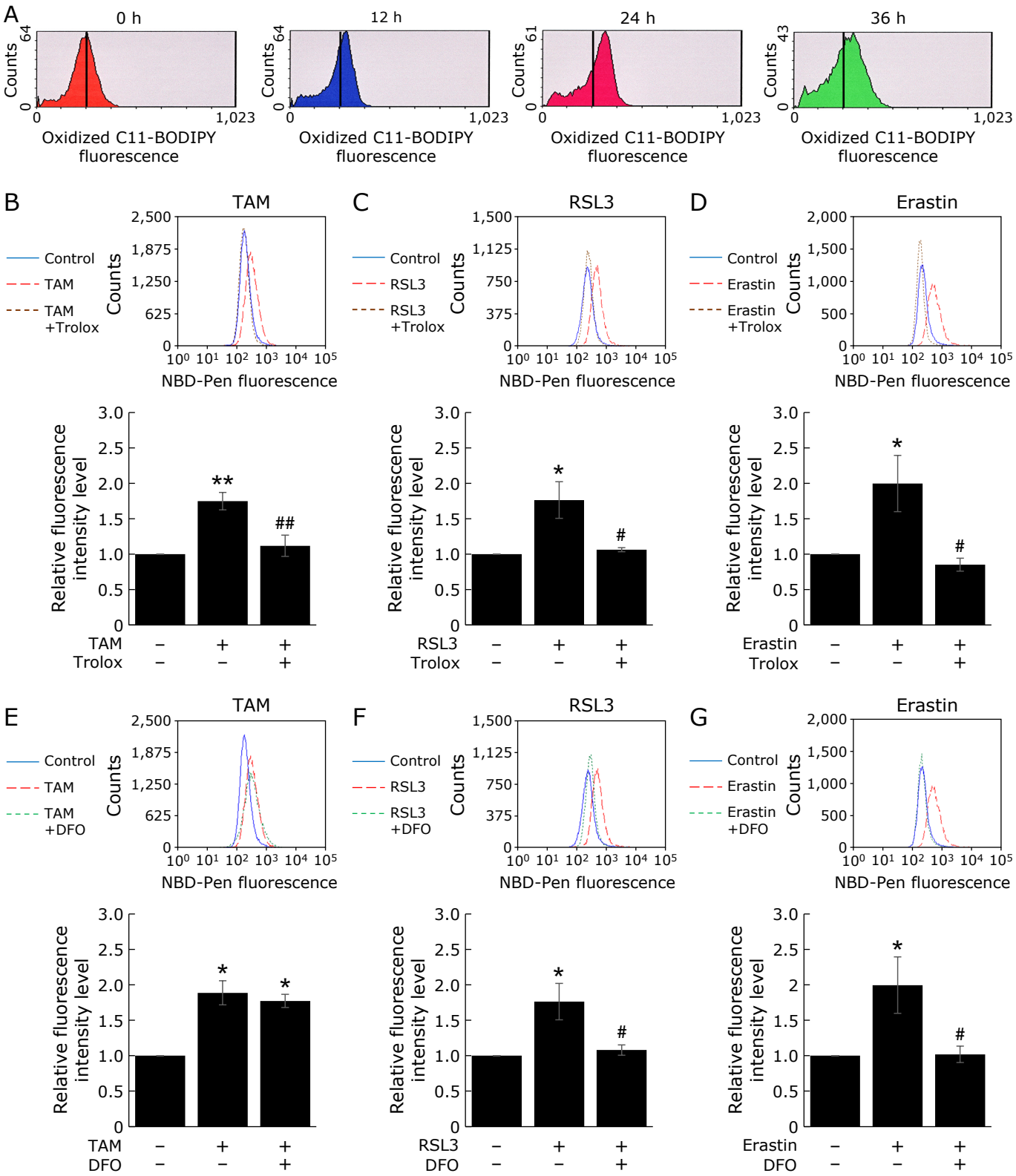

Fig. 3. Tamoxifen-induced GPx4-deficient cell death of ETK1 cells caused by iron-independent lipid peroxidation. (A) Time-dependent detection of lipid peroxidation after the addition of 1 μM Tamoxifen in Tamoxifen-inducible GPx4-deficient cells (ETK1) using 4 μM BODIPY™ 581/591 C11 by flow cytometry. (B–G) Effects of 600 μM Trolox and 100 μM DFO on lipid peroxidation induced through treatment with 1 μM RSL3 for 3 h (C, F), 1 μM erastin for 7 h (D, G), and 1 μM Tamoxifen (TAM) for 24 h (B, E). Lipid peroxidation was detected at each point using the fluorescent lipid radical probe, NBD-Pen, by flow cytometric analysis. (B–D) Typical analysis diagram for flow cytometry and results of the relative fluorescence intensity regarding the effect of Trolox on Tamoxifen (TAM) induced lipid peroxidation (B), RSL3 induced lipid peroxidation (C) and erastin induced lipid peroxidation (D). (E–G) Typical analysis diagram for flow cytometry and results of the relative fluorescence intensity regarding the effect of DFO on Tamoxifen (TAM) induced lipid peroxidation (E), RSL3 induced lipid peroxidation (F) and erastin induced lipid peroxidation (G). The values represent the mean ± SE (each group, $n = 3$). *p<0.05 vs ETK1 cells with no inhibitor (control), **p<0.01 vs ETK1 cells with no inhibitor (control), $^{\#}p$<0.05 vs each cell death inducer treated ETK1 cells, $^{\#\#}p$<0.01 vs each cell death inducer treated ETK1 cells.

doi: 10.3164/jcbn.23-101

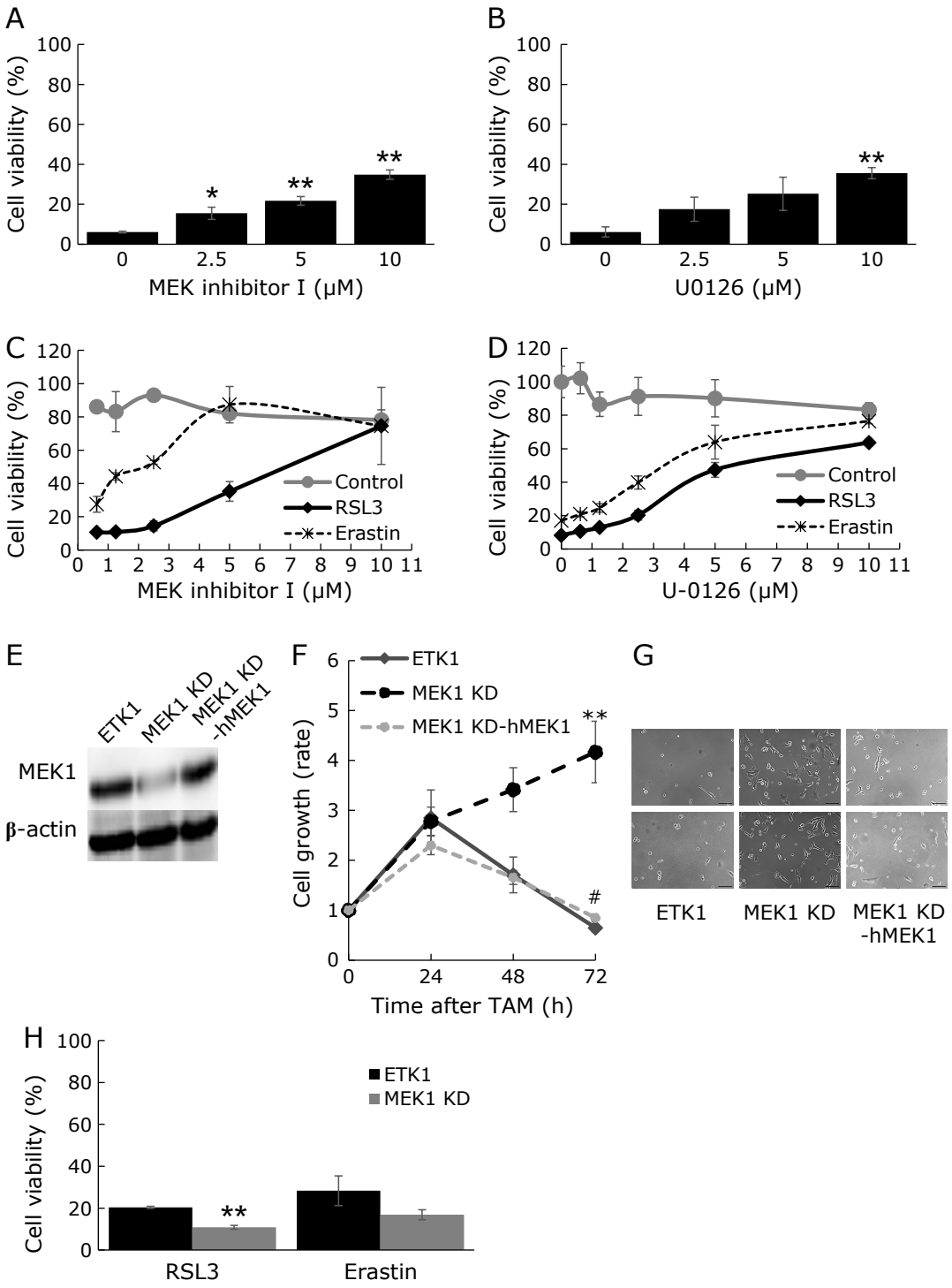

Fig. 4. MEK1 inhibition suppresses Tamoxifen-induced GPx4-deficient cell death. (A, B) Effects of MEK inhibitors on Tamoxifen-inducible GPx4-deficient cell death in ETK1 cells. Cell viability was assessed 72 h after the addition of 1 μM Tamoxifen with various concentrations of MEK inhibitor I (A) and U0126 (B) in ETK1 cells. The values represent the mean ± SE (each group, $n = 3$). *$p<0.05$ vs TAM treated ETK cells with no inhibitor, **$p<0.01$ vs TAM treated ETK cells with no inhibitor. (C, D) Effects of MEK inhibitors on RSL3- or erastin-induced ferroptosis in ETK1 cells. Cell viability was assessed 24 h after the addition of 1 μM RSL3 or 1 μM erastin with various concentrations of MEK inhibitor I (C) and U0126 (D) in ETK1 cells. Controls represent the cell viability (toxicity) when only MEK inhibitors are added and cultured for 24 h. The values represent the mean ± SE (each group, $n = 3$). (E–H) MEK1 knockdown inhibited Tamoxifen-inducible GPx4-deficient cell death, but not RSL3- or erastin-induced ferroptosis. (E) Expression of MEK1 protein in ETK1 (control) cells, MEK1 knockdown (KD) cells, and hMEK1 transfected MEK1 KD cells by immunoblot analysis with anti-MEK1 and anti β-actin antibodies. (F, G) Cell Growth rates (F) and two representative images at 72 h (G) of ETK1 cells, MEK1 KD cells and human MEK1 re-transfected with MEK1 KD cells every 24 h after the addition of 1 μM Tamoxifen. The scale indicates 100 μm. The values represent the mean ± SE (each group, $n = 3$). **$p<0.01$ vs Tam treated ETK1 cells, $^{\#}p<0.05$ vs Tam-treated MEK1 KD cells. (H) Cell viability was assessed 24 h after the addition of RSL3 or erastin to EKT1 cells (control) and MEK1 KD cells. The values represent the mean ± SE (each group, $n = 3$). **$p<0.01$ vs RSL3 treated ETK1 cells.

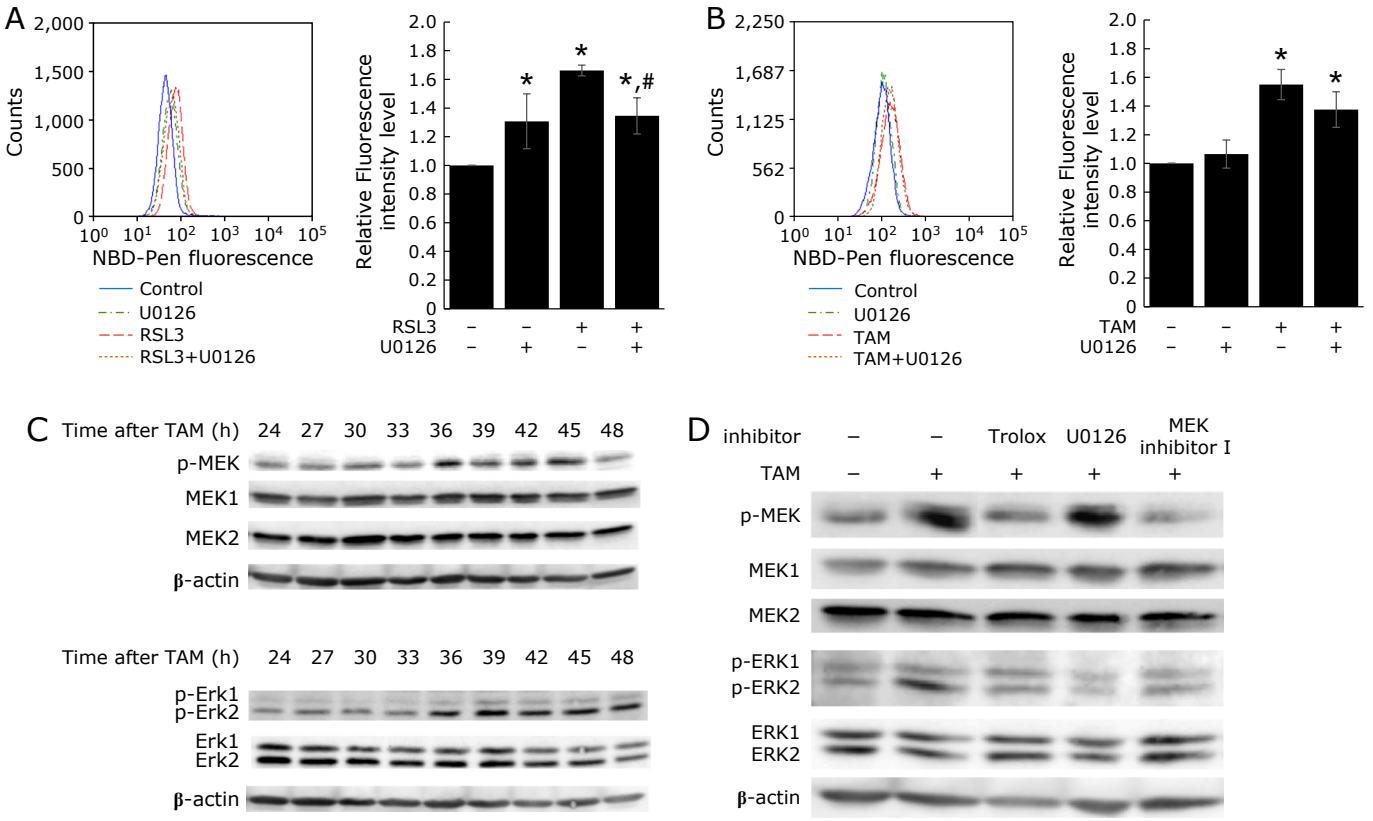

Fig. 5. MEK/ERK2 pathway downstream functions of lipid peroxidation in Tamoxifen-inducible GPx4-deficient cell death in ETK1 cells. (A) Effects of U0126 on lipid peroxidation at 3 h in RSL3-induced ferroptosis in ETK1 cells. Lipid peroxidation was detected at 3 h after the addition of 1 μM RSL3 with or without 10 μM U0126 using the fluorescent lipid radical probe, NBD-Pen, by flow cytometric analysis. (B) Effects of U0126 on lipid peroxidation at 24 h in Tamoxifen-inducible GPx4-deficient cell death in ETK1 cells. Lipid peroxidation was detected at 24 h after the addition of 1 μM Tamoxifen with or without 10 μM U0126 using the fluorescent lipid radical probe, NBD-Pen, by flow cytometric analysis. The values represent the mean ± SE (each group, $n = 3$). *$p<0.05$ vs ETK1 cells with no inhibitor (control), #$p<0.05$ vs RSL3-treated ETK1 cells. (C) Immunoblot analysis showing that MEK/ERK2 phosphorylation occurs from 36 to 48 h after lipid peroxidation at 24 h in Tamoxifen (TAM)-inducible GPx4-deficient cell death in ETK1 cells. (D) Immunoblot analysis showing that 300 μM Trolox, 10 μM U0126, and 10 μM MEK inhibitor I inhibited MEK/ERK2 phosphorylation 39 h after the addition of 1 μM Tamoxifen (TAM).

GPx4-deficient cell death, we examined whether the phosphorylation of MEK/ERK occurs downstream of lipid peroxidation in Tamoxifen-inducible GPx4-deficient cell death using immunoblotting with phospho-MEK1/2 antibody and phospho-ERK1/2 antibody. Interestingly, MEK1/2 was phosphorylated from 36 h to 45 h after the addition of Tamoxifen, and ERK2 was also phosphorylated from 36 h to 48 h after the addition of Tamoxifen, but ERK1 was not phosphorylated (Fig. 5C). U0126 or MEK inhibitor I are known to inhibit ERK phosphorylation through MEK without or with inhibition of MEK phosphorylation. Both MEK inhibitors remarkably suppressed ERK2 phosphorylation at 39 h after the addition of Tamoxifen (Fig. 5D). On the other hand, treatment with the antioxidant Trolox inhibited MEK and ERK2 phosphorylation after the addition of Tamoxifen, which indicates that MEK/ERK2 was activated from 36 h to 48 h after lipid peroxidation at 24 h in Tamoxifen-inducible GPx4-deficient cell death.

MEK1/2 can phosphorylate ERK1 and ERK2, and we investigated whether the ERK 1 and 2 specific inhibitors could suppress Tamoxifen-inducible GPx4-deficient cell death in ETK1 cells. Pluripotin, Ulixertinib, and AZD0364 were ERK1, ERK1/2, and ERK2 selective inhibitors, respectively. Ulixertinib and AZD0364 weakly suppressed Tamoxifen-inducible GPx4-deficient cell death in a dose-dependent manner, but pluripotin did not, thus indicating that ERK2 might be partially involved in Tamoxifen-inducible GPx4-deficient cell death (Fig. 6A–C). However, pluripotin, ulixertinib, and AZD0364 could not inhibit RSL3- or erastin-induced ferroptosis. (Fig. 6D–F). These results suggest that the MEK1/ERK2 pathway functions downstream of lipid peroxidation in Tamoxifen-inducible GPx4-deficient cell death, an iron-independent lipid peroxidation-induced cell death, in ETK1 cells. This was a cell death pathway that was distinct from RSL3-or erastin-induced ferroptosis.

Discussion

Ferroptosis inducers such as RSL3 and erastin are known to quickly induce iron-dependent lipid peroxidation-triggered cell death.[7,8] In the established Tamoxifen-inducible GPx4-deficient cells (ETK1 cells), RSL3 and erastin-induced lipid peroxidation and cell death were effectively inhibited by the iron chelator DFO, the antioxidant Trolox, and Fer-1 (Fig. 1F, Fig. 2A and B, Fig, 3C, D, F and G). This indicates that we confirmed that RSL3 and erastin induce ferroptosis, an iron-dependent lipid peroxidation-triggered cell death, in ETK1 cells. RSL3 is known to bind GPx4 and induce the loss of GPx4 activity.[8] On the other hand, erastin inhibits the Cystin transporter, resulting in the depletion of glutathione (GSH), a reducing substance required for GPx4 activity.[7] Because GPx4 KO mice are embryonic lethal[1] and the depletion of GPx4 in MEF cells, such as Pfa1 cells,[6,8] induces lipid peroxidation-triggered cell death,[2,6,8] it has been considered that RSL3- and erastin-induced ferroptosis and GPx4-

doi: 10.3164/jcbn.23-101

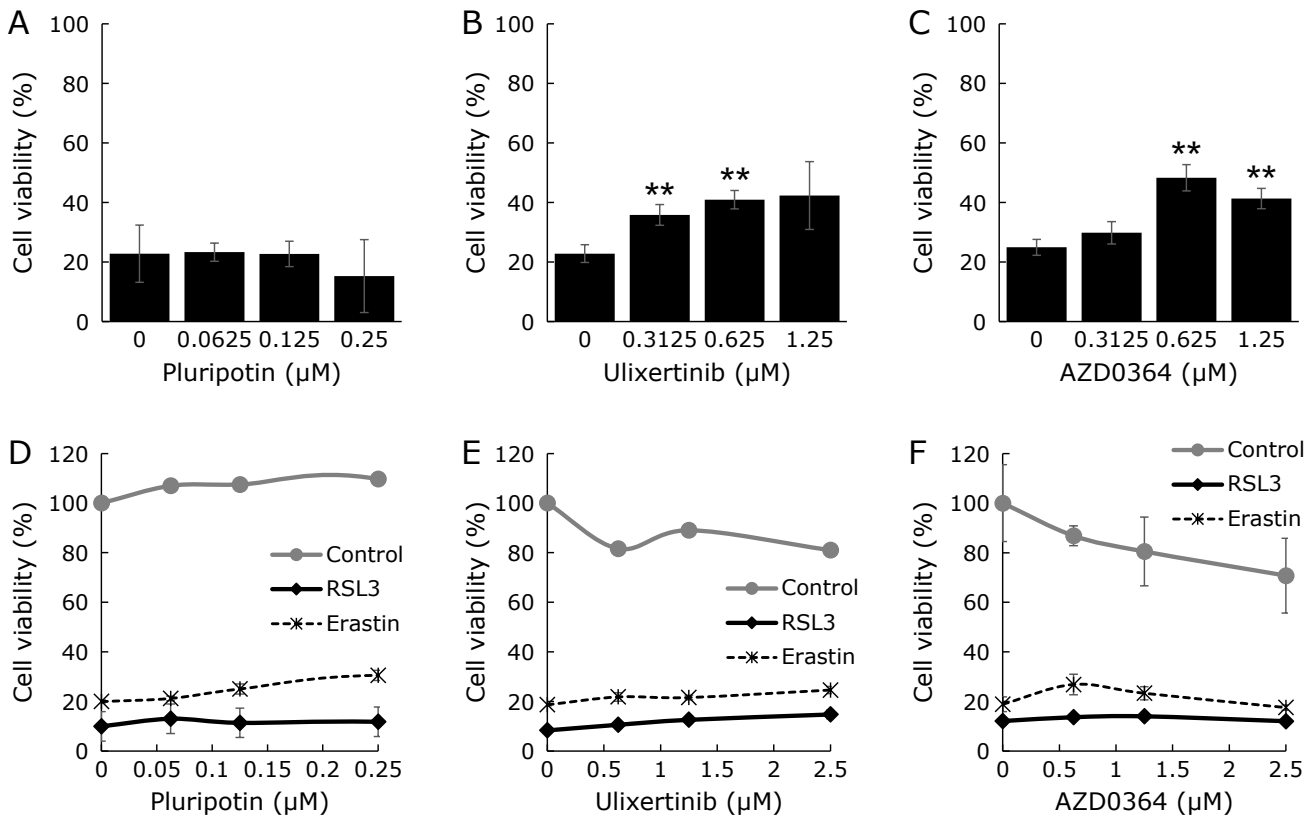

Fig. 6. ERK2 selective inhibitor inhibits Tamoxifen-inducible GPx4-deficient cell death but not RSL3- or erastin-induced ferroptosis in ETK1 cells. (A–C) Cell viability was assessed 72 h after the simultaneous addition of 1 μM Tamoxifen with various concentrations of ERK inhibitors in ETK1 cells. Pluripotin (ERK1 inhibitor) (A), Ulixertinib (ERK1/2 inhibitor) (B), and AZD0364 (ERK2 inhibitor) (C) were used as the ERK-specific inhibitors. The values represent the mean ± SE (each group, $n = 3$). $^{**}p<0.01$ vs TAM treated ETK1 cells with no inhibitor. (D–F) Cell viability was assessed 24 h after the simultaneous addition of RSL3 or erastin with various concentrations of Pluripotin (D), Ulixertinib (E), and AZD0364 (F). Controls represent the cell viability (toxicity) when only ERK inhibitors are added and cultured for 24 h. The values represent the mean ± SE (each group, $n = 3$).

deficient cell death through GPx4 genome disruption occur via the same cell death mechanism.[7,8]

As shown in Fig. 1F, 2A, and 3C and F, RSL3-induced lipid peroxidation occurs in an iron-dependent manner at 3 h, followed by cell death at 12–24 h in the established ETK1 cells. It takes 9–21 h from lipid peroxidation to cell death. However, in GPx4-deficient cell death induced through disruption of the GPx4 genome by the addition of Tamoxifen in the established ETK1 cells, lipid peroxidation occurs at 24 h in accordance with the decrease in GPx4 protein level after the addition of Tamoxifen and cell death occurs after 72 h, as shown in Fig. 1A–C and Fig. 3A, B and E. It takes 48 h from lipid peroxidation to cell death in ETK1 cells. Because RSL3-induced ferroptosis and Tamoxifen-induced GPx4-deficient cell death differ greatly in the time of cell death from lipid peroxidation in ETK1 cells, we hypothesized that in the established ETK1 cells, both cell death types may be caused by different mechanisms, although they both target the same molecule, GPx4. We found that lipid peroxidation induced by RSL3 occurred in an iron-dependent Fenton reaction, whereas lipid peroxidation in GPx4-deficient cell death was generated in an iron-independent manner in ETK1 cells (Fig. 3B, C, E and F). In ETK1 cells, Tamoxifen-inducible GPx4-deficient cell death occurs slowly after iron-independent lipid peroxidation but not ferroptosis. In ferroptosis, the iron-mediated Fenton reaction enhances lipid peroxidation and quickly induces cell death. However, iron-independent lipid peroxidation is considered to be an enzyme-mediated lipid peroxidation reaction that results in slow cell death, suggesting that oxidized lipids may function as cell death signals. Further studies are required to identify the lipid-oxidizing enzymes and to analyze the mechanism of slow cell death induced by iron-independent lipid peroxidation.

To clarify the mechanism of iron-independent lipid peroxidation-induced cell death through GPx4 gene disruption, we screened the chemical inhibitor library against several enzymes and the inhibitors of the known cell death types to suppress Tamoxifen-induced GPx4-deficient cell death in ETK1 cells. We showed that Tamoxifen-induced GPx4-deficient cell death cannot be inhibited by known cell death inhibitors of apoptosis, necroptosis, or autophagic cell death (Fig. 2F). We found that MEK1/2 inhibitors, such as U0126 and MEK inhibitor I, could suppress Tamoxifen-induced GPx4-deficient cell death in a dose-dependent manner in ETK1 cells (Fig. 4A and B). However, MEK inhibitors were also reported to inhibit erastin- and RSL3-induced cell death during the initial chemical library screening.[7–10] The screening experiments showed that erastin- and RSL3-induced cell death only occurred in cancer cells in which the RAS/RAF/MEK pathway with mutant RAS^{V12} was activated and did not inhibit cell death in normal cells. Therefore, it is reported that cell death in cancer cells by erastin is suppressed by inhibiting the growth signals that are involved in lipid peroxidation and activated by RAS/RAF/MEK with MEK inhibitors.[9] Erastin bound to mitochondrial voltage-dependent anion channels other than xCT (cystin transporter), a ferroptosis regulator, resulted in oxidative cell death.[9] In the ferroptosis pathway, the inhibitory mechanism of MEK inhibitors is not well understood.

We confirmed that U0126 and MEK inhibitor I could inhibit

erastin- and RSL3-induced ferroptosis in a dose-dependent manner in ETK1 cells (Fig. 4C and D). Additionally, flow cytometric analysis using NBD-Pen, a lipid radical detector, indicated that U0126 significantly inhibited the lipid peroxidation generated by RSL3 at 3 h, suggesting that the RAS/RAF/MEK growth signal involved in lipid peroxidation was inhibited by the MEK inhibitor (Fig. 5A). Surprisingly, U0126 could not suppress lipid peroxidation at 24 h in Tamoxifen-inducible GPx4 deficient cell death in ETK1 cells, thus indicating that MEK activation occurs after lipid peroxidation at 24 h (Fig. 5B).

Immunoblot analysis revealed that the enhancement of MEK1/2 phosphorylation was observed from 36 h to 45 h after the addition of Tamoxifen, and ERK2 phosphorylation was also observed from 36 h to 48 h, but ERK1 was not phosphorylated in Tamoxifen-inducible GPx4-deficient cell death (Fig. 5C and D). This indicates that MEK/ERK2 phosphorylation was observed after lipid peroxidation at 24 h in Tamoxifen-inducible GPx4-deficient cell death. Moreover, MEK1/2 and ERK2 phosphorylation at 39 h were significantly inhibited by the addition of Tamoxifen with the antioxidant Trolox in Tamoxifen-inducible GPx4-deficient cell death, indicating that the activation of MEK1/2 and ERK2 might be involved after lipid peroxidation in Tamoxifen-inducible GPx4-deficient cell death (Fig. 5C and D). Tamoxifen-inducible GPx4-deficient cell death was inhibited by MEK1 knockdown, and Tamoxifen-inducible GPx4-deficient cell death was restored with the re-transfection of human MEK1 in MEK1 knockdown cells, indicating that MEK1 is required for GPx4-deficient cell death after lipid peroxidation (Fig. 4E–G). Surprisingly, RSL3- or erastin-induced ferroptosis could not be suppressed in MEK1 knockdown cells (Fig. 4H). MEK activates ERK1 and ERK2 through phosphorylation. In GPx4-deficient cell death, we observed increased phosphorylation of ERK2 after lipid peroxidation; therefore, we examined whether cell death could be inhibited by the ERK1, ERK2, and ERK1/2 selective inhibitors pluripotin, AZD0364, and Ulixertinib, respectively. The ERK2-selective inhibitor and ERK1/2 inhibitor weakly inhibited GPx4-deficient cell death, but the ERK1-selective inhibitor failed to do so (Fig. 6). However, neither RSL3- nor erastin-induced ferroptosis was suppressed by any of the ERK inhibitors and was not inhibited by MEK1 knockdown. These results indicate that the MEK-ERK pathway is not involved in RSL3- or erastin-induced ferroptosis. For RSL3- and erastin-induced ferroptosis, it may be possible to induce cell death if either MEK1 or MEK2 enzymes can be activated. Another possibility is that enzymes other than MEK1/2, which are inhibited by MEK inhibitors, may be involved in the induction of ferroptosis. A detailed analysis of the function of MEK in ferroptosis by RSL3 or erastin remains to be performed.

In this study, we showed for the first time that the MEK1/ERK2 pathway is involved in the execution of iron-independent lipid peroxidation-mediated cell death as a downstream function of lipid peroxidation in ETK1 cells. The RAF/MEK/ERK pathway plays a pivotal role in cell cycle progression and cell survival, and its deregulation often causes tumorigenesis.[23,24] However, sustained activation of this pathway can also induce cell cycle arrest or various cell death types.[25,26] Sustained and extreme energetic stress promotes a switch to isoform-specific MEK1/ERK2 signaling for cell death.[27] In melanoma and lung cancer cells, death induced through drug withdrawal was preceded by a specific ERK2-dependent phenotype switch.[28] It is very interesting to note that the MEK1/ERK2 pathway is also included in cell death in an iron-independent lipid peroxidation-dependent manner in this study.

To date, the molecular mechanisms of ferroptosis have been analyzed mainly using Pfa1 cells, established by Seiler *et al.*[6] as Tamoxifen-induced GPx4-deficient MEF cells. They initially reported that GPx4-deficient cell death in Pfa1 cells was 12/15-LOX-dependent and AIF-mediated cell death[6]. Furthermore, Kagan *et al.*[11] reported that 15-LOX-dependent oxidation of PE triggered RSL3-induced and GPx4-deficient ferroptosis in Pfa1 cells. Dolls *et al.*[12,13] identified ACSL4 and FSP1 as ferroptosis regulators using Pfa1 cells. However, these ferroptosis regulators were all molecules that could alter the sensitivity to lipid peroxidation and function upstream of lipid peroxidation in the ferroptosis pathway, while signaling molecules that function downstream of lipid peroxidation in ferroptosis remain largely unknown. Recently, Hirata *et al.*[29] reported that increased membrane permeability to cations is a crucial step in the execution of ferroptosis and identified Piezo1, TRP channels, and the Na^+/K^+ ATPase as targets or effectors of oxidized lipids in the membrane.

Both Pfa1 and ETK1 cells were Tamoxifen-induced GPx4-deficient MEF cells. Although Pfa1 cells express 12/15-LOX that could directly oxidize phospholipid in the membrane,[6,11] the established ETK1 cells in this study did not express 12/15-LOX (data not shown), which suggests a different mechanism of lipid peroxidation due to GPx4-deficiency. GPx4-deficient cell death in ETK1 cells was not suppressed by AIF knockdown, and time-lapse analysis showed that the necrosis-like swelling observed in Pfa1 cells during ferroptosis was not observed in the ETK cells (unpublished personal communication). These results suggest that cell death might occur differently in Pfa1 and ETK1 cells in the absence of GPx4. Disruption of the GPx4 gene alone in ETK1 cells did not induce an iron-mediated lipid peroxidation (Fig. 3B and E). Because RSL3 can bind to other proteins, in addition to GPx4,[8] it may have the ability to stimulate iron release as well as inhibit GPx4 activity.

In the present study, using the established Tamoxifen-inducible GPx4-deficient cells, ETK1 cells, we found that iron-independent lipid peroxidation due to GPx4-deficiency induced a novel cell death type "lipoxytosis" that involved the activation of MEK1/ERK2 after lipid peroxidation. The regulatory mechanisms of lipoxytosis are currently being investigated.

Author Contributions

HI designed the study. KT performed all of the experiments. HI, MM, SH, and AE performed a part of the experiments and analyzed and interpreted the data. KIY supplied the information and knowledge regarding NBD-Pen, for the detection of lipid peroxidation. TKumagai, SY, and TKoumura provided technical advice for the experiments and analysis. KT wrote the first draft of the article. HI reviewed and edited the article.

Acknowledgments

We would like to acknowledge Kumiko Konishi-Doi, Nobuko Ohkawa, Inoru Kobayashi, Ryuya Kobayashi, Maho Morita and Sae Yahagi for their valuable technical support. This study was supported in part by Grants-in-Aid from Scientific Research (B) (JP20H03385), (A) (JP20H00493), (S) (JP23H05481), and Early-Career Scientists (JP23K14351) from the Japan Society for the Promotion of Science (JSPS) KAKENHI, and Grant-in-Aid for JSPS Fellows (JP21J15474), and AMED under Grant Number (JP22gm0910013), Grants-in-Aid for Transformative Research Areas (A) Sulfur biology (22H05575), and Kitasato University Research Grant for Young Researcher and Ono Medical Research Foundation. We would like to thank Enago for English language review and editing.

Abbreviations

AIF	apoptosis inducing factor
COPD	chronic obstructive pulmonary disease
DFO	deferoxamine
ERK	extracellular signal-regulated kinase

doi: 10.3164/jcbn.23-101

Fer-1	ferrostatin-1
GPx4	glutathione peroxidase 4
GPx4-loxP TG	glutathione peroxidase 4 genome loxP containing transgene
LOX	lipoxygenase
MEK1	mitogen-activated protein kinase kinase 1
NCOA4	nuclear receptor coactivator 4
shRNA	short hairpin RNA
SOD	superoxide dismutase

Conflict of Interest

No potential conflicts of interest were disclosed.

References

1 Imai H, Hirao F, Sakamoto T, *et al*. Early embryonic lethality caused by targeted disruption of the mouse PHGPx gene. *Biochem Biophys Res Commun* 2003; **305**: 278–286.
2 Imai H. New strategy of functional analysis of PHGPx knockout mice model using transgenic rescue method and Cre-LoxP system. *J Clin Biochem Nutr* 2010; **46**: 1–13.
3 Imai H, Hakkaku N, Iwamoto R, *et al*. Depletion of selenoprotein GPx4 in spermatocytes causes male infertility in mice. *J Biol Chem* 2009; **284**: 32522–32532.
4 Ueta T, Inoue T, Furukawa T, *et al*. Glutathione peroxidase 4 is required for maturation of photoreceptor cells. *J Biol Chem* 2012; **287**: 7675–7682.
5 Imai H, Matsuoka M, Kumagai T, Sakamoto T, Koumura T. Lipid peroxidation-dependent cell death regulated by GPx4 and ferroptosis. *Curr Top Microbiol Immunol* 2017; **403**: 143–170.
6 Seiler A, Schneider M, Förster H, *et al*. Glutathione peroxidase 4 senses and translates oxidative stress into 12/15-lipoxygenase dependent- and AIF-mediated cell death. *Cell Metab* 2008; **8**: 237–248.
7 Dixon SJ, Lemberg KM, Lamprecht MR, *et al*. Ferroptosis: an iron-dependent form of nonapoptotic cell death. *Cell* 2012; **149**: 1060–1072.
8 Yang WS, SriRamaratnam R, Welsch ME, *et al*. Regulation of ferroptotic cancer cell death by GPX4. *Cell* 2014; **156**: 317–331.
9 Yagoda N, von Rechenberg M, Zaganjor E, *et al*. RAS-RAF-MEK-dependent oxidative cell death involving voltage-dependent anion channels. *Nature* 2007; **447**: 864–868.
10 Yang WS, Stockwell BR. Synthetic lethal screening identifies compounds activating iron-dependent, nonapoptotic cell death in oncogenic-RAS-harboring cancer cells. *Chem Biol* 2008; **15**: 234–245.
11 Kagan VE, Mao G, Qu F, *et al*. Oxidized arachidonic and adrenic PEs navigate cells to ferroptosis. *Nat Chem Biol* 2017; **13**: 81–90.
12 Doll S, Proneth B, Tyurina YY, *et al*. ACSL4 dictates ferroptosis sensitivity by shaping cellular lipid composition. *Nat Chem Biol* 2017; **13**: 91–98.
13 Doll S, Freitas FP, Shah R, *et al*. FSP1 is a glutathione-independent ferroptosis suppressor. *Nature* 2019; **575**: 693–698.
14 Mishima E, Ito J, Wu Z, *et al*. A non-canonical vitamin K cycle is a potent ferroptosis suppressor. *Nature* 2022; **608**: 778–783.
15 Nakamura T, Hipp C, Santos Dias Mourão A, *et al*. Phase separation of FSP1 promotes ferroptosis. *Nature* 2023; **619**: 371–377.
16 Yoshida M, Minagawa S, Araya J, *et al*. Involvement of cigarette smoke-induced epithelial cell ferroptosis in COPD pathogenesis. *Nat Commun* 2019; **10**: 3145.
17 Tadokoro T, Ikeda M, Ide T, *et al*. Mitochondria-dependent ferroptosis plays a pivotal role in doxorubicin cardiotoxicity. *JCI Insight* 2020; **5**: e132747.
18 Abe K, Ikeda M, Ide T, *et al*. Doxorubicin causes ferroptosis and cardiotoxicity by intercalating into mitochondrial DNA and disrupting Alas1-dependent heme synthesis. *Sci Signal* 2022; **15**: eabn8017.
19 Jiang X, Stockwell BR, Conrad M. Ferroptosis: mechanisms, biology and role in disease. *Nat Rev Mol Cell Biol* 2021; **22**: 266–282.
20 Liang D, Minikes AM, Jiang X. Ferroptosis at the intersection of lipid metabolism and cellular signaling. *Mol Cell* 2022; **82**: 2215–2227.
21 Imai H, Suzuki K, Ishizaka K, *et al*. Failure of the expression of phospholipid hydroperoxide glutathione peroxidase in the spermatozoa of human infertile males. *Biol Reprod* 2001; **64**: 674–683.
22 Yamada K, Mito F, Matsuoka Y, *et al*. Fluorescence probes to detect lipid-derived radicals. *Nat Chem Biol* 2016; **12**: 608–613.
23 Chambard JC, Lefloch R, Pouysségur J, Lenormand P. ERK implication in cell cycle regulation. *Biochim Biophys Acta* 2007; **1773**: 1299–1310.
24 Balmanno K, Cook SJ. Tumour cell survival signalling by the ERK1/2 pathway. *Cell Death Differ* 2009; **16**: 368–377.
25 Subramaniam S, Unsicker K. ERK and cell death: ERK1/2 in neuronal death. *FEBS J* 2010; **277**: 22–29.
26 Cagnol S, Chambard JC. ERK and cell death: mechanisms of ERK-induced cell death—apoptosis, autophagy and senescence. *FEBS J* 2010; **277**: 2–21.
27 Shin S, Buel GR, Wolgamott L, *et al*. ERK2 mediates metabolic stress response to regulate cell fate. *Mol Cell* 2015; **59**: 382–398.
28 Kong X, Kuilman T, Shahrabi A, *et al*. Cancer drug addiction is relayed by an ERK2-dependent phenotype switch. *Nature* 2017; **550**: 270–274.
29 Hirata Y, Cai R, Volchuk A, *et al*. Lipid peroxidation increases membrane tension, Piezo1 gating, and cation permeability to execute ferroptosis. *Curr Biol* 2023; **33**: 1282–1294.e5.